

# Effects of doping profile and temperature on the solar cell performances

Asma Benchiheb  
Faculté de médecine, Université de  
Constantine 3, Algérie  
Laboratoire des Microsystèmes et  
Instrumentation. Département  
d'Electronique, Constantine 1,  
asmabenchiheb@yahoo.fr

Nedjouda Benchiheb  
Ecole National Supérieur  
d'hydraulique, Blida  
nedjouabenchiheb@yahoo.fr

Yasmina Saidi  
Département de Physique, Université  
de Constantine 1, Algérie  
saidiyas09@yahoo.fr

Farida Hobar  
Département d'électronique, Universit  
d' Oum El Bouaghi  
Laboratoire des Microsystèmes et  
Instrumentation. Département  
d'Electronique, Constantine 1  
hobarfarida@yahoo.fr

**Abstract**—In this paper, an optimization of the structure of a silicon solar cell is presented. This study takes into account the effects of temperature and doping level of each region of the device. As the simulation with the COMSOL software allowed us to demonstrate the link between the technological structure of an N + NP type solar cell and the various characteristics and parameters obtained at the output when it is subjected to a polarization. Thus, we considered different doping levels and thicknesses of the N + layer. It has been observed that the effects of temperature are negligible for low doping levels of the N + layer. However, in heavy doping, the benefit of reducing its thickness below 0.018  $\mu\text{m}$  is demonstrated, especially for the high temperature operating range. Concerning the base, we observed that its thickness must be maintained in the order of 100  $\mu\text{m}$ .

**Keywords**—Solar Cell, optimization, temperature

## I. INTRODUCTION

Currently, the efficiency of solar cells is in the order of 20% to 30%. In order to improve it, various solutions have been provided such as, for example, the use of multi-junctions [1,2]. However, the disadvantage of this solution is its relatively high price compared to that of uni-junction cells technologies.

To improve the efficiency of solar cells in the production of electricity, several models based on the techniques of emitter region optimizing [3-5] are proposed. Therefore, this quest made it possible to achieve great breakthroughs in the emitters design philosophy as well as to lead to solar cells exhibiting increasingly interesting yields, especially among those which are based on the use of silicon in their production.

In this paper, we present an optimization of silicon solar cell structure taking into consideration the operating

## II. THE STUDIED STRUCTURE

The general structure and doping profile of the silicon solar cell studied are presented on Fig. 1 and table I. This one consists of three layers :

- One P-type layer forming the substrate and doped with boron.
- One phosphorus doped N-type layer with a Gaussian profile
- One layer of N + type also doped with phosphorus and a Gaussian profile.

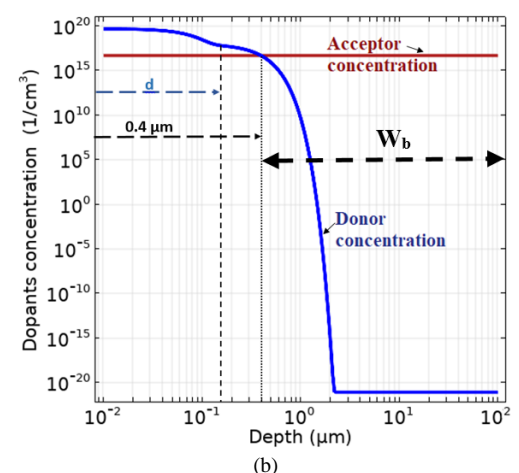
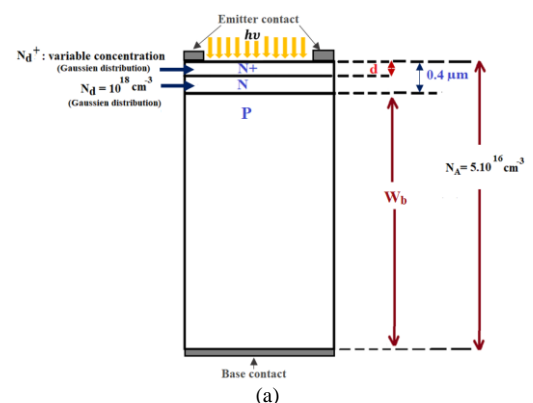


Fig.1. Structure of the silicon solar : a) general structure, b) doping profile

TABLE I. PHYSICAL PARAMETERS VALUES

Solar cell parameter	n-p (conventional)	n <sup>+</sup> - n -p
Surface concentration	N <sub>d</sub> =1. 10 <sup>18</sup> cm <sup>-3</sup>	N <sub>d</sub> <sup>+</sup> is variable
Emitter doping profile	Gaussian W <sub>Nd</sub> = 0.4 μm	Gaussian on Gaussian W <sub>Nd<sup>+</sup></sub> = d
Base doping concentration Base thickness	N <sub>a</sub> = 5. 10 <sup>16</sup> cm <sup>-3</sup> W <sub>b</sub>	

### III. DESCRIPTION OF NUMERICAL MODEL

The equations governing the transport phenomena in the solar cell are [6]:

$$\text{div} \cdot (\epsilon \cdot \overrightarrow{\text{grad}V}) = -\rho \quad (1)$$

$$g_n - r_n = -\frac{1}{q} \cdot \overrightarrow{\nabla} \cdot \overrightarrow{J}_n \quad (2)$$

$$g_p - r_p = \frac{1}{q} \cdot \overrightarrow{\nabla} \cdot \overrightarrow{J}_p \quad (3)$$

$$\overrightarrow{J}_n = q \cdot n \cdot \mu_n \cdot \overrightarrow{E} + q \cdot D_n \cdot \overrightarrow{\nabla} n \quad (4)$$

$$\overrightarrow{J}_p = q \cdot p \cdot \mu_p \cdot \overrightarrow{E} - q \cdot D_p \cdot \overrightarrow{\nabla} p \quad (5)$$

With

- ρ : The charges density;
- ε : Material permittivity
- J<sub>n,p</sub> : Current density for electrons, holes;
- D<sub>n,p</sub> : Diffusion constant for electrons, holes
- μ<sub>n,p</sub> : Mobility of electrons, holes;
- KB : Boltzmann constant
- T : The temperature
- r<sub>n,p</sub> : recombination term for electrons, holes
- g<sub>n,p</sub> : photo generation term for electrons, holes

The recombination term r<sub>n,p</sub> takes into account Shockley-Read-Hall (SHR) type recombination and Auger effect [6-8].

Under illumination, the photo generation rate for each wavelength λ is calculated by the equation [9]:

$$G(\lambda \cdot x) = \alpha(\lambda) \cdot I_o(\lambda) \cdot e^{-\alpha(\lambda) \cdot x} \quad (6)$$

Where I<sub>o</sub>(λ) is the intensity of photons at the cell surface (x = 0), I<sub>o</sub>(λ,x) the intensity of photons at point x and α(λ) the absorption coefficient at λ wavelength.

The total photo generation rate is the integral of G(x) over all wavelengths forming the solar spectrum

### IV. RESULTS AND DISCUSSIONS

Fig.2 and Fig. 3 show respectively the variations of the light-generated current density (or photocurrent density), ΔJ<sub>phl</sub>, and the Variation of the increase in the conversion efficiency, Δη<sub>1</sub>, as functions of the thickness d, for different surface doping levels and temperatures.

ΔJ<sub>phl</sub>=J<sub>ph</sub>-J<sub>ph0</sub> and Δη<sub>1</sub>=η-η<sub>0</sub> where J<sub>ph</sub> and η are respectively the n<sup>+</sup>- n -p light-generated current density and the conversion efficiency and J<sub>ph0</sub> the light-generated current density without the N<sup>+</sup> layer i.e with a 0.4 μm type N emitter and a metal contact directly taken on this layer. For this case, W<sub>b</sub> is set to 100 μm

Fig. 2 demonstrates that overall, the increase in the surface doping of the N + region induces a growth of the photocurrent. However, for a given value of this surface doping and over a small thickness d (d < d<sub>o</sub>), first, we observe an increase in the photocurrent but from a certain limit of d<sub>o</sub>, this one decreases. Thus, for a surface doping less than 5.10<sup>19</sup> cm<sup>-3</sup>, d<sub>o</sub> is in the order of 0.08 μm but for surface doping greater than 5.10<sup>19</sup> cm<sup>-3</sup>, d<sub>o</sub> is in the order of 0.03 μm.

Regarding the effects of temperature, its influence is not remarkable until the surface doping level exceeds 10<sup>19</sup>cm<sup>-3</sup>. Indeed, from this limit, an increase in temperature induces a decrease in the photocurrent. In addition, this phenomenon is even more accentuated when the thickness of the layer N +, d, increases.

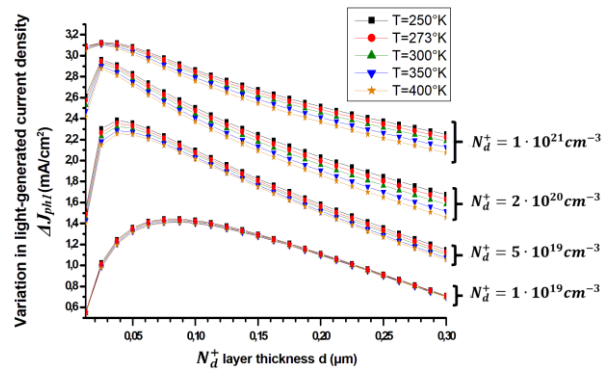


Fig.2. Variation of the increase in the light-generated current density with a high-low junction emitter versus n+-layer thickness for different surface doping concentration N<sub>d</sub><sup>+</sup> and temperatures.

Regarding the conversion efficiency, Fig.3 shows that, like the case of photocurrent, the influence of temperature is small when the doping level of the order of 10<sup>19</sup> cm<sup>-3</sup> (or less).

However, for average doping surface concentration (5.10<sup>19</sup>cm<sup>-3</sup> ≤ Nd < 2.10<sup>21</sup> cm<sup>-3</sup>), the increase in temperature leads to a decrease in the Δη for thicknesses d in the order of 0.03 μm but for greater thicknesses (d > 0.1 μm), the variation of this factor is very small.

For high doping levels of the order of 10<sup>21</sup> cm<sup>-3</sup>, a net decrease in the variation of the conversion efficiency is observed for thicknesses d in order of 0.018 μm. This factor stabilizes when d exceeds 0.15μm.

Thus, at high temperature and doping levels, the thickness of the layer must be kept low to ensure good performance.

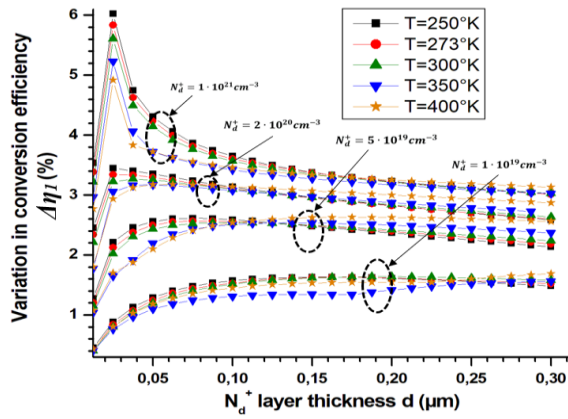


Fig.3. Variation of the increase in the conversion efficiency with a high-low junction emitter versus n+-layer thickness for different surface doping concentration  $N_d^+$  and temperature.

In order to study the influence of the base thickness,  $W_b$ , on the cell current and its efficiency, we consider  $N_d^+ = 2 \cdot 10^{20} \text{cm}^{-3}$ ,  $d = 0.02 \mu\text{m}$  but with  $W_b$  variable. We also put :  $\Delta\eta_2 = \eta - \eta_0$  and  $\Delta J_{ph2} = J_{ph} - J_{ph0}$  where  $\eta_0 = \eta$  (for  $W_b = 0.1 \mu\text{m}$ ) and  $J_{ph0} = J_{ph}$  (for  $W_b = 0.1 \mu\text{m}$ )

Fig. 4, 5 and 6 show that the variations of the current and the efficiency as well as the open circuit voltage of the cell increase rapidly with the thickness as long as  $W_b \leq 100 \mu\text{m}$ . These effects are due to photo generation phenomena of electron-hole pairs which occur more and more as the base widens. However, when  $W_b$  exceeds  $100 \mu\text{m}$ , these growths slow down to become almost constant because in this case, less light manages to cross the thick base thus limiting the photo-generation.

Regarding the effects of temperature, the variation of the latter does not have much influence on the photo-current. However, its increase induces a decrease in the open-circuit voltage. This explains the decrease in the variation in injection efficiency with temperature.

From these curves, we can deduce that for a good optimization of the structure, the thickness of the base must be chosen in the order of  $100 \mu\text{m}$ .

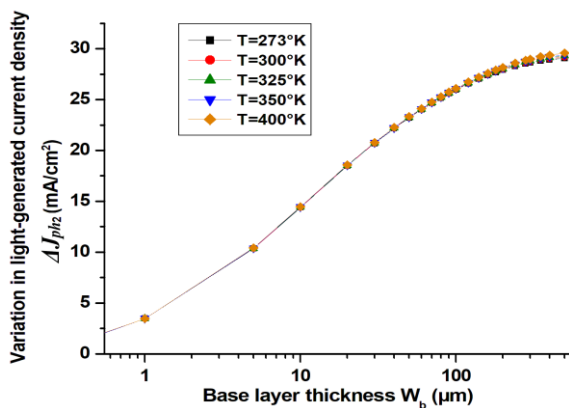


Fig.4. Variation of the increase in the light-generated current density with a high-low junction emitter versus base thickness  $W_b$  and temperature.

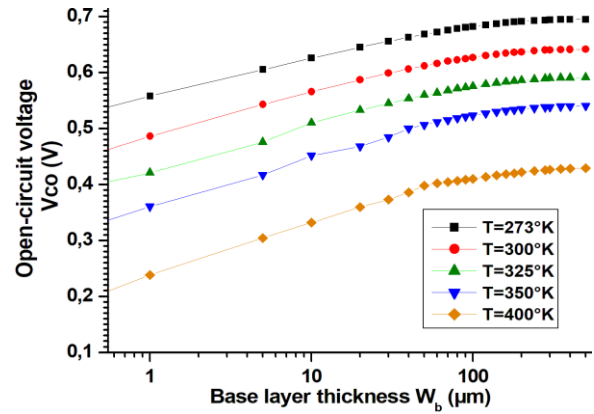


Fig.5. Open-circuit voltage versus base thickness  $W_b$  and temperature.

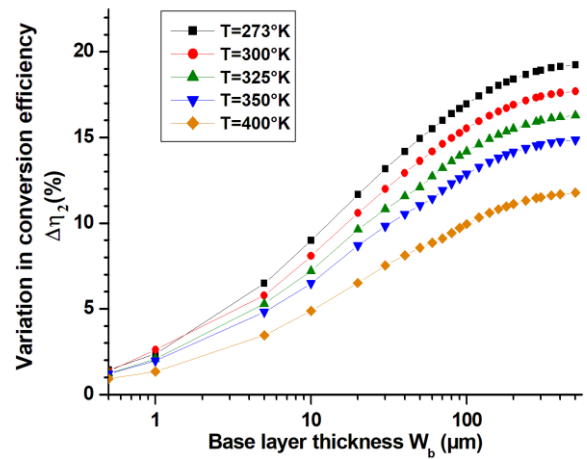


Fig.6. Variation of the increase in the conversion efficiency with a high-low junction emitter versus base thickness  $W_b$  and temperature.

## V. CONCLUSION

In order to optimize the solar cell structure, the study of its electrical behaviour shows that the thickness of the base must be in the order of  $100 \mu\text{m}$ . Regarding the emitter region, for high temperature operation, the thickness of the N+ region must be kept very low (of the order of  $0.018 \mu\text{m}$ ) for high doping levels exceeding  $10^{21} \text{cm}^{-3}$ . However, for regions of average doping surface concentration ( $5 \cdot 10^{19} \text{cm}^{-3} \leq N_d^+ < 2 \cdot 10^{21} \text{cm}^{-3}$ ), the thickness must be of the order of  $0.3 \mu\text{m}$ . For low level doping ( $N_d^+ < 5 \cdot 10^{19} \text{cm}^{-3}$ ), the temperature variation does not have much effect.

## REFERENCES

- [1] A. Mumtaz M. Milanova, I. Sandall, K. Cheetham, Z. Cao, M. Cao, G. Piana, N. Fleck, L., Phillips, "GaAsSbN for Multi-Junction Solar Cells," 2020 47th IEEE Photovoltaic Specialists Conference (PVSC), 2020, pp. 1799-1803.
- [2] A. Verma and A. Pethe, "Modelling and Analysis of Multi-Junction Photovoltaic Cells," 2020 IEEE 17th India Council International Conference (INDICON), 2020, pp. 1-6.
- [3] M. Shadab Siddiqui, B. K. Pant, A. K. Saxena, Shivangi and S. Chandril, "An analysis of Passivated emitter and rear contact (PERC) cell and module," 2019 IEEE 46th Photovoltaic Specialists Conference (PVSC), 2019, pp. 0334-0338.
- [4] S. Kim, H. Park, D. Phong Pham, Y. Kim S. Kim E.C. Cho Y. Cho, " Design of front emitter layer for improving efficiency in silicon heterojunction solar cells via numerical calculations," *Optik*, 2021, vol. 235, pp. 1-9.
- [5] B.K. Ghosh, A. M. Khairul, A. Afshah, I. Saad, A. I. A. Rani and S. K. Ghosh, "Analysis of emitter layer diverse effects on electrical performance for prospective Si hybrid solar cell," 5th IET

International Conference on Clean Energy and Technology (CEAT2018), 2018, pp. 1-4

- [6] A. Benchiheb, F. Hobar, " Modelling of the active defects influence on the electrical characteristics of an SiGe-HBT," Elsevier, ChineseJournal of Physics, 2017, vol. 55 pp. 1453-1465.
- [7] Silvaco, Atlas User's Manual-Device simulation software. Santa Clara, CA,2010, Ch. 3.
- [8] S. M. Sze, " Physics of semiconductor devices ", 2nd ed., John Wiley & Sons, 1981.
- [9] A.K. Singh, J. Tiwari, A. Yadav, R.K. Jha, " Analysis of Si/SiGe heterostructure solar cell", Journal of energy, vol. 2014 pp. 1-7.